The Rv0805 Gene from *Mycobacterium tuberculosis* Encodes a 3′,5′-Cyclic Nucleotide Phosphodiesterase: Biochemical and Mutational Analysis†

Avinash R. Shenoy,‡ Nandini Sreenath,‡ Marjetka Podobnik,§ Miroslav Kovačevič,§ and Sandhya S. Visweswariah*,‡

Department of Molecular Reproduction, Development and Genetics, Indian Institute of Science, Bangalore 560012, India, and National Institute of Chemistry, SI-1001 Ljubljana, Slovenia

Received June 28, 2005; Revised Manuscript Received October 4, 2005

ABSTRACT: *Mycobacterium tuberculosis* is an important human pathogen and has developed sophisticated mechanisms to evade the host immune system. These could involve the use of cyclic nucleotide-dependent signaling systems, since the *M.* tuberculosis genome encodes a large number of functional adenylyl cyclases. Using bioinformatic approaches, we identify, clone, and biochemically characterize the Rv0805 gene product, the first cyclic nucleotide phosphodiesterase identified in *M. tuberculosis* and a homologue of the cAMP phosphodiesterase present in *Escherichia coli* (*cpdA*). The Rv0805 gene product, a class III phosphodiesterase, is a member of the metallophosphoesterase family, and computational modeling and mutational analyses indicate that the protein possesses interesting properties not reported earlier in this class of enzymes. Mutational analysis of critical histidine and aspartate residues predicted to be essential for metal coordination reduced catalytic activity by 90−50%, and several mutant proteins showed sigmoidal kinetics with respect to Mn in contrast to the wild-type enzyme. Mutation of an asparagine residue in the GNHD motif that is conserved throughout the metallophosphoesterase enzymes almost completely abolished catalytic activity, and these studies therefore represent the first mutational analysis of this class of phosphodiesterases. The Rv0805 protein hydrolyzes cAMP and cGMP in vitro, and overexpression in *Mycobacterium smegmatis* and *E. coli* reduces intracellular cAMP levels. The presence of an orthologue of Rv0805 in *Mycobacterium leprae* suggests that the Rv0805 protein could have an important role to play in regulating cAMP levels in these bacteria and adds an additional level of complexity to cyclic nucleotide signaling in this organism.

Mycobacterium tuberculosis is probably one of the most devastating human pathogens known, being singly responsible for the largest number of deaths worldwide due to an infectious disease (*1*). Specific genes encoded in its genome could not only alter pathways within the bacteria but also modulate host response and therefore dictate pathogenicity. Most interestingly, the *M. tuberculosis* genome encodes a large number of genes that bear striking sequence, biochemical, and structural similarity to signaling proteins encoded by eukaryotes (*2*). These include not only protein kinases and protein phosphatases but also nucleotide cyclases and proteins containing cAMP/cGMP binding domains. This suggests that either the cNMP produced in the bacterium could modulate its own gene expression or secreted cNMP could alter the host's signaling pathways (*3*, *4*). Several mycobacterial nucleotide cyclases are indeed found to possess robust adenylyl cyclase (and in one case a low level of guanylyl cyclase) activity (*5*−*10*). Recent structural information on these mammalian-like signaling proteins has revealed subtle differences in their properties in comparison with their mammalian counterparts (*10*, *11*).

The large number of functional nucleotide cyclases encoded in mycobacterial genomes points toward the importance of cAMP in the physiology of these organisms, and it is likely that the generation of cNMPs is finely controlled in these bacteria. Cyclic AMP and cGMP levels are also modulated by degradation through the action of phosphodiesterases (PDEs) (*12*). This hydrolysis of cyclic nucleotides to 5′-AMP can be accomplished by enzymes that differ significantly in primary amino acid sequence, and therefore PDEs can be categorized into three classes (I−III) (*13*, *14*). The class I PDEs are so far the only ones characterized in higher eukaryotes and have been extensively studied at the biochemical and structural level (*12*). The class II enzymes have been identified in only a few organisms such as yeast, *Dictyostelium*, and *Vibrio* (*14*). The third class was identified in *Escherichia coli* as the regulator of the lactose operon and is called the Icc or CpdA protein (*15*). This class of enzymes has remained largely unexplored, and a related enzyme from *Haemophilus* has been identified but has not been purified or biochemically characterized (*16*).

In this study, utilizing bioinformatic approaches and extensive biochemical and mutational analyses, we have discovered a novel protein in *M. tuberculosis*, which represents the only cNMP PDE identifiable in this organism. This enzyme is the product of the Rv0805 gene and is similar

† This work was supported by grants from the Department of Biotechnology, Government of India, to the Indian Institute of Science under the Proteomics Program, the Council for Scientific and Industrial Research, New Delhi, India, and the Slovenian Research Agency, J4-6463 (for M.P.) and P1-0034 (for M.K.).

* To whom correspondence should be addressed. Tel: +9180-22932542. Fax: +9180-23600999. E-mail: sandhya@mrdg.iisc.ernet.in.

‡ Indian Institute of Science.

§ National Institute of Chemistry.

10.1021/bi0512391 CCC: $30.25
Published on Web 11/05/2005

Table 1: Oligonucleotides Used in This Study[a]

	primer name and sequence	plasmid generated
PCR	Rv0805fwd: GCACCTCTCGAGCATAGACTTAGGGCCGCG Rv0805rvs: AGAAGGCGGCCGCGGACGTCAGTCGACG	pPRO-Rv0805$^{1-318}$
	pPRO-NheINdeI-fwd: CACACAGGGCTAGCCATATGTCGTACTACCATC pPRO-rvs: ATCAGACCGCTTCTGCGTTCTG	pSD5-P_{hsp60}-Rv0805$^{1-318}$
mutagenesis	D21A: CTCTTACATATCAGCGCTACTCATCTCATCGGGGGG	pPRO-Rv0805$_{D21A}$
	H23A: CGATCCCCCCCGATGAGCGCTGTGTCGCTGATATGTAAG	pPRO-Rv0805$_{H23A}$
	D66A: CGGCGATTTGGCCGCTAAGGGCGAACCCGCGGCATACCGCAAG	pPRO-Rv0805$_{D66A}$
	N97A: GCGCCGAGCTGGTCTGGGTGATGGGTGCCCACGACGACCGGG	pPRO-Rv0805$_{N97A}$
	H169A: CGGAATCGGCGGATGAGCCAGCGCTAAAATGGTGCCGTCCG	pPRO-Rv0805$_{H169A}$
	H207A: GTCGAGTAGTGCAGGGCCCCGGCTAAAATGGCGCGAACGTC	pPRO-Rv0805$_{H207A}$

[a] The Rv0805fwd and Rv0805rvs primer sets were used for PCR amplification of the Rv0850 gene from the genomic DNA. pPRO-NheINdeI-fwd and pPRO-rvs were also used for PCR amplification of Rv0805 and cloning into pSD5-P_{hsp60}-Sm1647CD. The other oligonucleotides were used for site-directed mutagenesis by a procedure described earlier (*22*).

in sequence to the class III PDEs but unique in its properties. Rv0805 is a member of the structurally related metallophosphoesterase (MPE)[1] family of enzymes, representatives of which include mammalian calcineurin and related protein serine/threonine phosphatases and the purple acid phosphatases (*17*−*19*). Therefore, the Rv0805 gene product adds another level of complexity to cAMP signaling in *M. tuberculosis* and perhaps other pathogenic mycobacteria.

MATERIALS AND METHODS

Computational Sequence Analysis. An RPS-BLAST search with the COG2129 entry (*20*) for the Icc-related group of proteins, on 339 sequences that represent the Metallphos entry (PF00149) in the Pfam database (*21*), identified only eight sequences above a stringent scoring cutoff of 10^{-8} as putative cyclic nucleotide PDEs. These were multiply aligned, and a ls profile HMM (CIII-PDE HMM) built using the HMMer suite (http://hmmer.wustl.edu/) was used to identify related proteins in the genomes of *M. tuberculosis* and related mycobacteria.

Cloning, Expression, and Mutagenesis of Rv0805. The Rv0805 gene was cloned for expression in *E. coli* based on the annotation of the *M. tuberculosis* genome by the Sanger Centre. A modified touchdown PCR was carried out using Rv0805fwd and Rv0805rvs primers (Table 1), for amplifying Rv0805. PCR was performed on 100 ng of genomic DNA of *M. tuberculosis* H37Rv with Taq DNA polymerase (Finnzymes, Finland) in the presence of 5% DMSO with the annealing temperature reducing by 0.5 °C/cycle from 60 to 48 °C and subsequently increasing it by 1 °C/cycle from 49 to 55 °C, followed by keeping it unchanged at 52 °C for 10 cycles. The extension time was kept constant throughout at 72 °C for 1.5 min. The fragment obtained following PCR was cloned into the *Sal*I and *Not*I sites of the pPROExHT-C vector (Invitrogen Life Technologies) to generate the plasmid pPRO-Rv0805$^{1-318}$, allowing the synthesis of a hexahistidine-tagged protein with a Tev protease cleavage site between the tag and Rv0805. The D21A, H23A, D66A, N97A, H169A, and H207A mutations were generated on the pPRO-Rv0805$^{1-318}$ plasmid using a single oligonucleotide based mutagenesis protocol (*22*). The sequences of the mutagenic oligonucleotides used for mutagenesis are provided in Table 1. All plasmids were sequenced in order to ascertain the presence of only the desired mutations (Macrogen).

Wild-type and mutant proteins were produced in the CodonPlus RP strain (Stratagene) of *E. coli* on induction using IPTG (500 μM) for 3 h at 37 °C. Cells were lysed by sonication in 50 mM Tris-HCl (pH 8.5), 5 mM 2-mercaptoethanol (2-ME), 100 mM NaCl, and 2 mM phenylmethanesulfonyl fluoride (PMSF), followed by centrifugation at 30000*g*. The supernatant was interacted with Ni-NTA beads (Qiagen) and the protein purified in a manner similar to that described earlier (*7*, *8*). Purified proteins were treated with 5 mM EDTA for 1 h at 4 °C and then desalted into 50 mM HEPES/NaOH (pH 8.5), 5 mM 2-ME, 50 μM EDTA, 50 mM NaCl, and 10% glycerol and stored in aliquots at −80 °C until further use in phosphodiesterase assays as described below. Purified proteins were subjected to SDS gel electrophoresis with standard protein molecular mass markers (β-galactosidase, 116 kDa; bovine serum albumin, 66 kDa; chicken egg ovalbumin, 45 kDa; lactate dehydrogenase, 35 kDa; and restriction endonuclease *Bsp*981, 25 kDa; MBI Fermentas).

Static Light Scattering and Inductively Coupled Plasma Mass Spectrometric (ICP-MS) Analysis. Protein purified from the Ni-NTA column was cleaved with Tev protease at 4 °C for 16 h in 50 mM Tris-HCl, pH 8.0, 50 mM NaCl, 5 mM 2-ME, and 10% glycerol. Tev protease and the remaining noncleaved Rv0805 were separated from the His-tag free Rv0805 by running the sample again over the Ni-NTA column after the protease cleavage. The nonbound fraction with Rv0805 was concentrated on Amicon Ultra-15 concentrators with 10 kDa cutoff (Millipore) before application onto the Superdex 200 10/30 gel filtration column (GE Healthcare). Static light scattering experiment was preformed on-line with the gel filtration column in 20 mM Tris-HCl, pH 8.0, 50 mM NaCl, and 5 mM 2-ME at a flow rate of 0.5 mL min^{-1}. Light scattering was performed on a Dawn-DSP multiangle laser photometer equipped with a He−Ne laser (λ_0 = 633 nm) and an Optilab-DSP interferometric refractometer (Wyatt Technology Corp.).

ICP-MS was carried out using an Agilent 4500 inductively coupled plasma mass spectrometer. Prior to ICP-MS analysis, the dimeric fraction of protein isolated from gel filtration on an AKTA FPLC system (GE Healthcare, Sweden) in 20 mM Tris-HCl, pH 8.0, 50 mM NaCl, and 2% glycerol was concentrated to >15 mg/mL. Concentrated protein solutions

[1] Abbreviations: bis(pNPP), bis(*p*-nitrophenyl phosphate); DEPC, diethyl pyrocarbonate; ICP-MS, inductively coupled plasma mass spectrometry; IPTG, isopropyl thiogalactopyranoside; MPE, metallophosphoesterase; PMSF, phenylmethanesulfonyl fluoride; pNPP, *p*-nitrophenyl phosphate; SDS, sodium dodecyl sulfate.

were brown in color, perhaps indicating the presence of Fe, and the protein was >90% pure as monitored by SDS gel electrophoresis (data not shown). For quantification of metal content in this protein, ~0.2 mL of solution containing purified protein (220 μM dimer, as determined by absorbance at 280 nm) was mineralized in a Milestone microwave oven in a mixture of 3 mL of nitric acid and 0.5 mL of hydrogen peroxide and was diluted with water to 15 mL prior the ICP-MS analysis. Calibration solutions for elements were matrix-matched. The following elements/isotopes were monitored: ^{24}Mg, ^{27}Al, ^{43}Ca, ^{53}Cr, ^{55}Mn, ^{57}Fe, ^{59}Co, ^{60}Ni, ^{63}Cu, ^{66}Zn, and $^{206-208}$Pb.

Homology Modeling. The Modeller suite (*23*) (version 7.7) was used for building a theoretical model, the templates for which were decided on the basis of hits obtained from a 3D-PSSM search (*24*) using the Rv0805 sequence as query. Three templates, i.e., chains B and C of the kidney bean PAP (PDB code 4kbp) (*25*), and regions from the Mre11 protein (PDB code 1ii7) (*26*) and the metal atoms from the sweet potato PAP (PDB code 1xzw) (*27*) were used. The sequence alignment used for building the homology model was similar to the one shown in Figure 1, except one change worth noting. The difference in the lengths of loops in Rv0805 compared to the templates necessitated the insertion of a two amino acid gap immediately after D63 in Rv0805 such that D66 was positioned on D169 from the kidney bean PAP and S54 in Mre11. Energy minimization of the optimized model built with default options in Modeller was carried out with the GROMOS96 implementation in the Swiss-PDB viewer (version 3.7) (*28*) and repeated after introduction of iron and manganese. Structure superposition for introducing metal atoms was performed using Dalilite (*29*). Panels shown in Figure 4 were created using PyMOL (www.pymol.org).

Preparation of Electrocompetent Mycobacterium smegmatis. Electrocompetent cells were prepared by growing *M. smegmatis* mc^2 155 in Middlebrook 7H9 containing 0.05% Tween 80 and 2% glucose for ~18 h and washing cells three times in ice-cold 10% glycerol solution. Cells were finally suspended in ~$^1/_{250}$th of the original culture volume and electroporated with ~300 ng of the pSD5-P_{hsp60} vector control or pSD5-P_{hsp60}-Rv0805$^{1-318}$ plasmid DNA with a single 2.5 kV pulse in a 0.2 cm cuvette (Bio-Rad) using a Bio-Rad gene pulser. Transformed cells were grown in Middelbrook's 7H9 containing 0.2% glycerol, 0.05% Tween 80, and 100 μg/mL kanamycin.

Overexpression of Rv0805 and Measurement of Intracellular cAMP Levels. Overexpression of Rv0805 in *M. smegmatis* was carried out using the pSD5 vector (*30*) containing the *hsp60* promoter, which was obtained from Prof. Anil K. Tyagi, University of Delhi. PCR was carried out on pPRO-Rv0805$^{1-318}$ as template using the pPRO-NheINdeI-fwd primer and pPRO-rvs primers (Table 1), which amplifies the Rv0805 gene along with the hexahistidine tag. The PCR product was cloned into *Nde*I−*Not*I sites of a pSD5-P_{hsp60} vector where the catalytic domain of MSMEG3786 had been cloned earlier (pSD5-P_{hsp60}-Sm1647CD; manuscript in preparation) to generate the plasmid pSD5-P_{hsp60}-Rv0805$^{1-318}$.

M. smegmatis cells transformed with pSD5-P_{hsp60}-Rv0805$^{1-318}$ plasmid were grown in Middlebrook's 7H9 containing 0.2% glycerol, 0.05% Tween 80, and 100 μg/mL kanamycin and lysed by bead beating for 1 min using 0.5 mm zirconium beads in 50 mM sodium acetate buffer (pH 4.6). Part of the lysate was used for protein estimation using commercial Bradford dye (Sigma-Aldrich), and the rest was placed in a boiling water bath for 5 min and cooled prior to estimation of cAMP by radioimmunoassay (*9*).

For Western blot analysis to monitor the expression of Rv0805 in *M. smegmatis*, cells were cultured as described above, and ~2×10^8 cells were subjected to four quick freeze−thaw cycles in liquid nitrogen in a buffer consisting of 25 mM Tris-HCl (pH 8.2), 1 mM EDTA, 5 mM 2-ME, 100 mM NaCl, and 4% SDS, followed by 15 pulses of sonication (U50 control sonicator; IKA Labrotechnik; 60−70% amplitude). Western blotting was carried out using the affinity-purified immunoglobulin fraction (100 ng/mL) purified from an antibody raised in rabbits against the purified Rv0805 protein.

RESULTS

Identification of a Novel Class III PDE in M. tuberculosis. Initial bioinformatic analysis was performed to identify homologues of the extensively studied class I and II PDEs, but these were not detected in *M. tuberculosis* (data not shown). However, with the conviction that the presence of a large number of functional nucleotide cyclases encoded in the *M. tuberculosis* genome would necessitate an efficient means of cyclic nucleotide degradation in this organism, we performed a search using our manually curated profile hidden Markov model (HMM) for the less well characterized class III PDEs. We thus were able to identify only a single gene, Rv0805, as a putative cAMP PDE in *M. tuberculosis* H37Rv. An identical protein could be found in the *M. tuberculosis* strain CDC1551 (MT0825) and *Mycobacterium bovis* (Mb0828). Importantly, an orthologue of Rv0805 was also detected in the *Mycobacterium leprae* (ML2210) genome, which is characterized by extensive gene loss and the presence of a number of pseudogenes. Interestingly, only more distant homologues could be found in *Mycobacterium avium* (MAP4220) and in the recently sequenced genome of *M. smegmatis* (MSMEG6576).

Rv0805 bears significant sequence similarity to the MPEs characterized from plants and higher mammals, with the core MPE domain in Rv0805 (residues ~15−210) containing critical catalytic residues required for phosphoester hydrolysis (Figure 1). This region of Rv0805 has ~31% identity with the Icc protein in *E. coli*, indicating that Rv0805 may function as a cyclic nucleotide phosphodiesterase.

The presence of an orthologue in *M. leprae* has been taken as evidence of this gene to be not nonessential (*31*). Since no detailed biochemical or structural information is available on any class III PDE to date, coupled with a lack of biochemical information on Rv0805 whose sequence showed interesting divergence from the metallophosphoesterases, we went on to study its biochemical properties in greater detail.

Biochemical Characterization of Rv0805. Rv0805 was expressed to high levels in *E. coli*, and SDS gel electrophoresis of the Ni-NTA purified protein showed the presence of minor bands of lower molecular weight which represented proteolytically degraded fragments, as monitored by Western blot analysis using an antibody raised to Rv0805 and peptide mass fingerprinting (data not shown). Gel filtration analyses

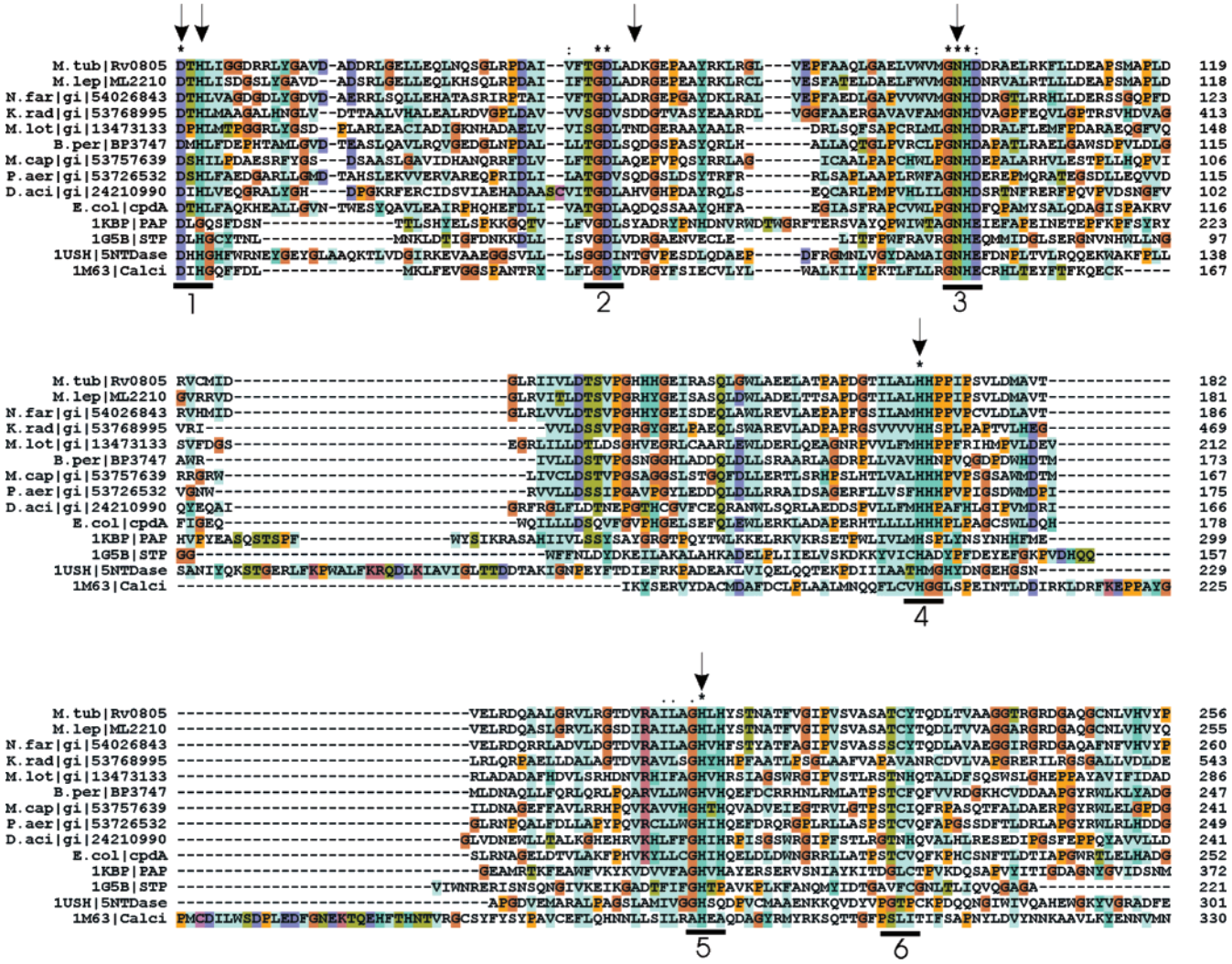

FIGURE 1: Sequence analyses of class III PDEs and MPEs. A multiple sequence alignment of Rv0805, putative class III PDEs, and MPEs spanning the MPE domain is shown. Residues in Rv0805 that have been mutated in this study are marked by arrows. Black lines with numbers indicate the six conserved motifs that are present in class III PDEs. Motifs 1−5 are conserved across MPEs. Abbreviations: B.per, *Bordetella pertussis*; D.aci, *Delftia acidovorans*; E.col, *Escherichia coli*; K.rad, *Kineococcus radiotolerans*; M.cap, *Methylococcus capsulatus*; M.lep, *M. leprae*; M.lot, *Mesorhizobium loti*; M.tub, *M. tuberculosis*; N.far, *Nocardia farcinica*; P.aer, *Pseudomonas aeruginosa.* GenBank identifiers or genome annotations have been used. PDB codes have been used for the kidney bean purple acid phosphatase (PAP), bacteriophage λ serine−threonine phosphatase (STP), *E. coli* 5′-nucleotidase (5NTDase), and human calcineurin (Calci).

with the purified protein revealed that the Rv0805 protein formed a stable dimer, with minor amounts of a monomeric species (Figure 2a). Static light scattering of the monomeric and dimeric fractions indicated molecular masses of 38500 Da ± 4% and 74500 ± 0.4%, respectively.

ICP-MS analysis of the purified dimeric protein showed that, per mole of protein, ~0.5 mol of Fe, ~0.15 mol of Mn, and ~0.05 mol each of Zn and Ni were bound. Across several experiments, we consistently found that Fe and Mn remain bound to the protein even after extensive treatment with 10 mM EDTA (data not shown), indicating a high-affinity interaction with metals. The specificity of the presence of these metals in Rv0805 was confirmed by analyzing the metal content of another protein (Precission protease), purified along similar lines. No Fe or Mn could be found associated with the protease (data not shown), indicating that these metals were specifically associated with Rv0805. Rv0805 is therefore likely to contain a binuclear metal center as seen in PAPs and related MPEs (*18*). The protein, however, as purified was not fully saturated with metal at its binuclear metal center, and it remains unclear at present why the metal occupancy of the isolated protein was so low, despite the apparent high affinity of the binding sites.

The MPE enzyme family contains proteins with either mono- or diesterase activities. Rv0805 was assayed at various pHs in the presence of Mn as added metal cofactor, using *p*-nitrophenyl phosphate (pNPP; a monoester) and bis-(*p*-nitrophenyl phosphate) [bis(pNPP); a diester] as substrates, and activity was highest in the pH range 8.5−9.5 (data not shown). The activities with bis(pNPP) and pNPP were 6.6 ± 0.07 and 0.017 ± 0.003 μmol of pNP produced min^{-1} (mg of protein)$^{-1}$, respectively, at pH 8.5, indicating that Rv0805 is clearly a phosphodiesterase due to the preferential (~400-fold higher) hydrolysis of the diester compound.

Catalytic activity of Rv0805 was enhanced on addition of Mg^{2+} or Mn^{2+}, whereas Fe^{2+}, Fe^{3+}, Zn^{2+}, Ni^{2+}, or Co^{2+} did not alter the activity of the enzyme (data not shown). As treatment with 2 mM 2,2′-dipyridyl, which selectively chelates Fe^{2+} ions, for 18 h at 4 °C did not affect the activity of Rv0805, the Fe in Rv0805 could be in the Fe^{3+} form (data not shown). Reaction kinetics were hyperbolic and did not indicate any cooperativity with respect to either the substrate

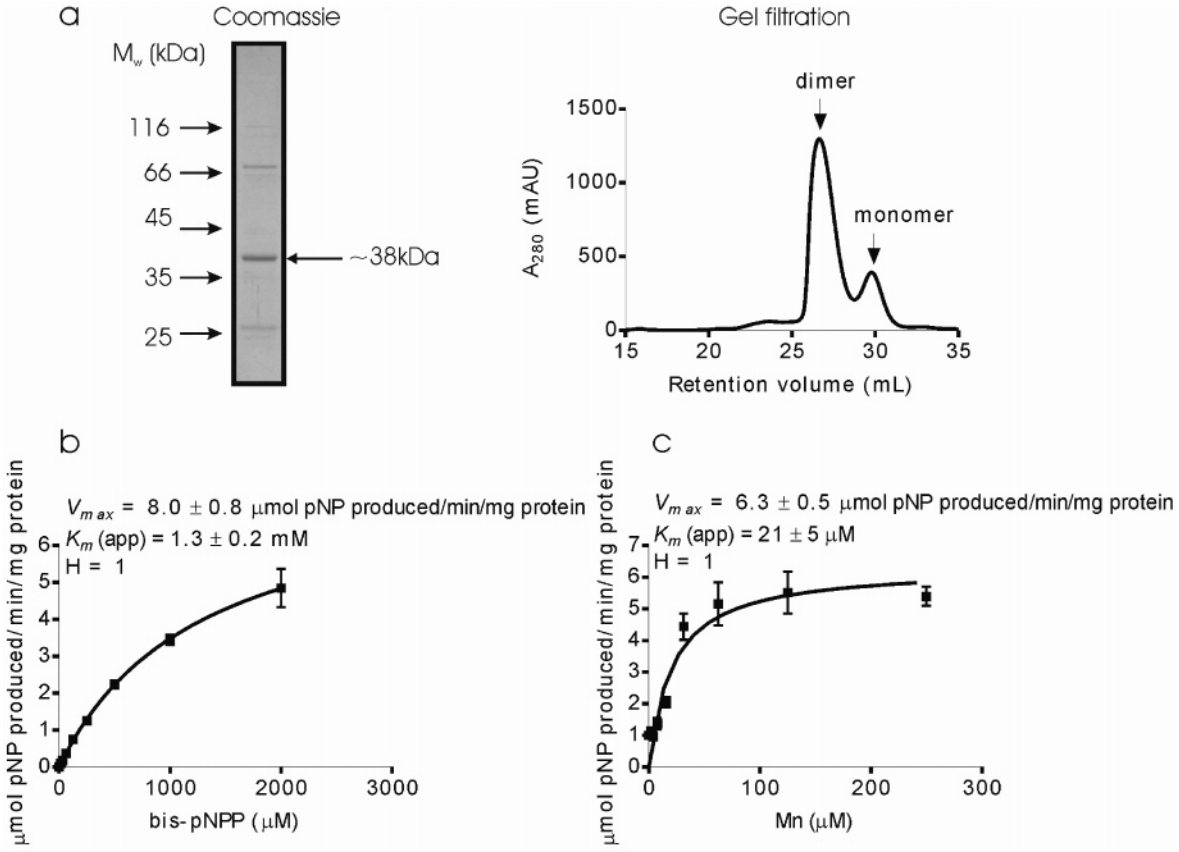

FIGURE 2: Expression and characterization of Rv0805. (a) Purified Rv0805 (~1 μg of protein) was separated by electrophoresis on a 12% SDS−polyacrylamide gel (left panel) and stained with Coomassie dye. Gel filtration analysis showing the presence of a dimer and a monomer is shown on the right. (b) Rv0805 was assayed in the presence of a fixed concentration of Mn (100 μM) and indicated concentrations of bis(pNPP). The mean ± SEM is shown ($n = 4$). (c) Rv0805 was assayed in the presence of a fixed concentration of bis(pNPP) (2 mM) and indicated concentrations of Mn. The mean ± SEM is shown ($n = 4$).

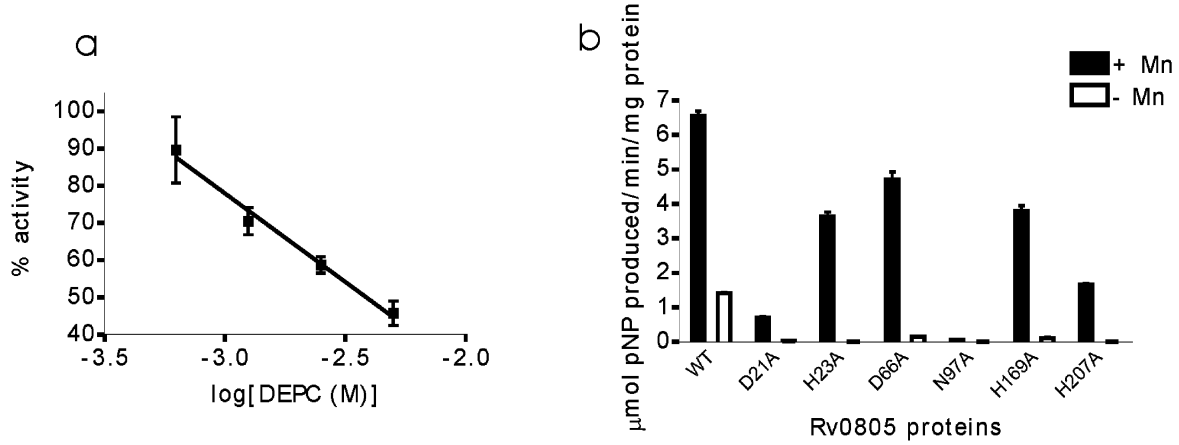

FIGURE 3: Mutational analyses of Rv0805. (a) Rv0805 protein was treated with the indicated concentrations of diethyl pyrocarbonate (DEPC) for 10 min at 4 °C and subsequently assayed in the presence of 2 mM bis(pNPP) and 100 μM Mn. The mean ± SEM is shown ($n = 4$). (b) Proteins were treated with EDTA as described in Materials and Methods and then assayed (~150 nM protein) in either the presence of absence of 100 μM Mn, using 2 mM bis(pNPP) as substrate.

or the cofactor (Figure 2b,c). The k_{cat} of the protein for bis-(pNPP) was ~250 /min.

No significant inhibition of activity was observed in the presence of sodium potassium tartarate, sodium phosphate, sodium pyrophosphate, sodium fluoride, imidazole (all at 1 mM), β-glycerophosphate (80 μM), phosphoserine (5 mM), and 100 μM calyculin or okadaic acid, all known inhibitors of the eukaryotic phosphoesterases. Activity was inhibited by 50%, however, in the presence of 1 mM sodium orthovanadate and 5 mM phosphotyrosine (data not shown), inhibitors of eukaryotic protein phosphatases, suggesting a unique conformation of the active site of Rv0805.

Mutational Analyses of Rv0805. Treatment of Rv0805 with diethyl pyrocarbonate (DEPC) reduced its activity by nearly 60%, suggesting the importance of histidines for catalysis (Figure 3a). Alanine mutants of conserved histidines predicted to be involved in metal coordination at each of the two metal centers (H23, H169, and H207) were made, which showed that $Rv0805_{H23A}$ and $Rv0805_{H169A}$ proteins had ~50% reduction in activity, while the $Rv0805_{H207A}$ mutant

Table 2: Kinetic Properties of Rv0805 Wild-Type and Mutant Proteins with Respect to Mn[a]

protein	V_{max}(app) [μmol of pNP produced min^{-1} (mg of protein)$^{-1}$]	$K_{(0.5)Mn}$(app) (μM)	Hill constant
Rv0805	6.3 ± 0.5	21 ± 5	1
$Rv0805_{D21A}$	0.7 ± 0.02	21 ± 1	4.1 ± 0.7
$Rv0805_{H23A}$	3.9 ± 0.2	53 ± 6	1
$Rv0805_{D66A}$	7.3 ± 0.1	72 ± 3	6.4 ± 1.2
$Rv0805_{H169A}$	4.0 ± 0.2	22 ± 2	1.7 ± 0.2
$Rv0805_{H207A}$	1.9 ± 0.1	62 ± 3	3.1 ± 0.4

[a] Proteins (~150 nM) were assayed in the presence of a fixed concentration of bis(pNPP) (2 mM) and varying concentrations of Mn. Results were analyzed by nonlinear regression curve fitting (using the Michaelis−Menten or the simplified Hill equation) in GraphPad Prism software. Values indicate the mean ± SEM ($n = 3$).

protein retained only ~25% activity (Figure 3b). Interestingly, in contrast to observations with the wild-type protein, EDTA treatment of the $Rv0805_{H23A}$, $Rv0805_{H169A}$, and $Rv0805_{H207A}$ proteins abolished the enzymatic activity completely, indicating that EDTA was able to strip the mutant proteins of the metal required for catalytic activity (Figure 3b). The apparent concentration of Mn for half-maximal activity ($K_{(0.5)}$) of the $Rv0805_{H23A}$ mutant increased, and sigmoidal kinetics were observed for the $Rv0805_{H169A}$ and $Rv0805_{H207A}$ mutants (Table 2). These results indicate that, in contrast to protein serine/threonine phosphatases, the role of these histidine residues is more subtle in Rv0805, since mutation of equivalent histidine residues in the λ phosphatase abolished activity completely (*32*).

Mutation of the conserved D21 residue to alanine led to a 90% loss in activity (Table 2). A critical asparagine residue is present in the GNHD motif (Figure 1) of MPEs which is involved in metal coordination (*17*), but the importance of this residue has not been tested by mutational analysis to date. Mutation of this asparagine residue to an alanine (N97A) resulted in a protein which retained less than 1% activity (Figure 3b), clearly indicating the critical requirement of this residue for catalytic activity in Rv0805 and, perhaps, in other MPEs.

In purple acid phosphatases (PAPs), a tyrosine residue is known to interact with the Fe^{3+} ion, which imparts the color to these proteins (*18*). Protein phosphatases contain an aspartate at this position which is also seen in Rv0805 (D66; Figure 1). Mutation of this aspartate residue to an alanine compromised the activity by ~25%. However, the $Rv0805_{D66A}$ mutant showed sigmoidal kinetics with respect to Mn (Table 2), again indicating the role of this residue in binding of the metals at the active site, thereby regulating the catalytic activity of the enzyme.

Homology Modeling of Rv0805. We performed homology modeling to investigate whether residues identified purely from sequence alignments could contribute to the formation of the active site in Rv0805. The crystal structures used for the modeling, based on hits from a 3D-PSSM search (*24*), were that of the kidney bean PAP and Mre11 nuclease (*25*, *26*). Both the chains of PAP and regions of Mre11 were used to generate the theoretical model. Rv0805 could adopt an overall structure similar to the MPEs with an internal symmetry where two β-sheets, containing four strands each, face each other and two α-helices lie on the outside in the repeating module (*33*) (Figure 4a). Metal atoms (Fe and Mn) were introduced from the recent crystal structure of the sweet potato PAP (*27*) and indicated that critical histidine and aspartate residues from Rv0805 are positioned in a manner that would allow for coordination of the two metals (Figure 4b). All critical residues that were mutated are in proximity to the metal atoms. The D21, H23, and D63 residues could be involved in coordinating Fe while D63, N97, H169, and H207 could be involved in coordinating Mn (Figure 4b).

Residues at the catalytic center could form hydrogen bonds with different residues or the main chain (Figure 4c). Asp 66 in Rv0805 is shown aligned with a tyrosine (Y167) present in PAPs that lies close to the Fe atom (*25*) in Figure 1. While modeling, however, due to the presence of a shorter loop in Rv0805 compared to the template, the D66 residue was modeled on the D169 residue in kidney bean PAP. The D66 residue, though not directly involved in binding the metals, may participate in polar interactions with the backbone region proximal to the GNH motif that contains the metal binding N97 residue, and therefore a loss of this interaction might be responsible for the high Hill coefficient on mutation of D66 (Table 2). The hydrogen bonding between the His residue in the GNH motif of MPEs with an aspartate residue derived from different nonequivalent sequence positions has been observed in several crystal structures (*34*). However, the histindine−asparate hydrogen bonding is not observed in the case of several PAPs including kidney bean PAP and Mre11 proteins that were used as templates for the modeling of Rv0805. Therefore, in the current model of Rv0805, D66 could form a hydrogen bond with the backbone peptide bond of D100 (Figure 4c) (*17*, *35*). In addition, D21 could form a polar interaction with the side chain of D63 and the backbone of H207. Given that D63 is the residue that binds both of the metals and H207 binds Mn and D21 itself binds Fe, mutation of D21 might destabilize the entire catalytic center. This is possibly the reason for the dramatic reduction in activity observed with the D21A mutant protein (Table 2).

Rv0805 Is a 3′,5′-Cyclic NMP Phosphodiesterase. We tested the ability of Rv0805 to hydrolyze 3′,5′-cyclic nucleotides, since Rv0805 shows sequence similarity to the *E. coli* Icc protein. As shown in Figure 5a significant cAMP phosphodiesterase activity was observed. Rv0805 hydrolyzed cAMP to 5′-AMP and not to adenosine, since we could detect liberated adenosine in the phosphodiesterase assay only after addition of 5′-nucleotidase (data not shown). Thus, Rv0805 lacks the monoesterase activity required to hydrolyze 5′-AMP.

Cyclic AMP phosphodiesterase activity appeared to be less compromised in the mutant proteins than was seen using bis-(pNPP) as substrate (Figure 5b). This perhaps is reflective of the high affinity of both the metal and cAMP for the enzyme, such that point mutations of single residues do not affect the activity of the enzyme significantly. This property is also distinct from the MPE superfamily, where mutations of residues at equivalent positions severely reduced catalytic activity against phosphoesters (*36*−*38*).

Cyclic GMP was also hydrolyzed by Rv0805, indicating that the selection of the cyclic nucleotide as substrate is not strict (data not shown). This is also evident from the open nature of the active site as seen in Figure 4a.

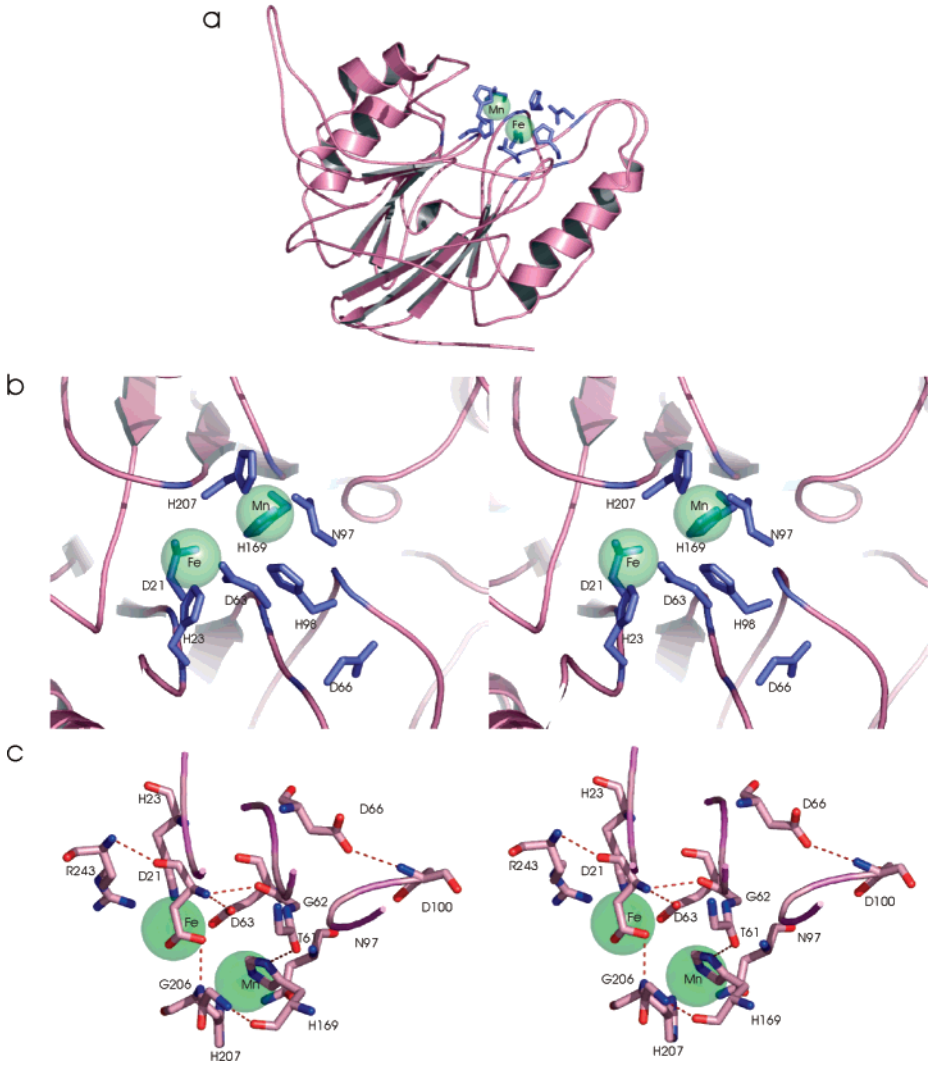

FIGURE 4: Homology modeling of Rv0805. (a) The theoretical model of Rv0805 shows the overall structure of the protein which has an internal symmetry with two opposing four-stranded β-sheets and α-helices on the outside. The metal atoms are shown as green spheres, and residues involved in coordinating the metal atoms are shown in blue. (b) The zoomed-in stereoview of the active site of Rv0805 is shown. Conserved residues are labeled, and metal atoms are shown as transparent green spheres. (c) A stereoview of the active site rotated ~180° along a horizontal axis as compared to the view shown in (b) is shown. Polar interactions between residues near the active site are shown as dashed red lines. Notice the interactions between D66 and backbone of D100 as well as the interactions between D21, H207, and D63. Colors used to represent atoms are as follows: carbon, pink; nitrogen, blue; oxygen, red; indicated metal atoms, green spheres.

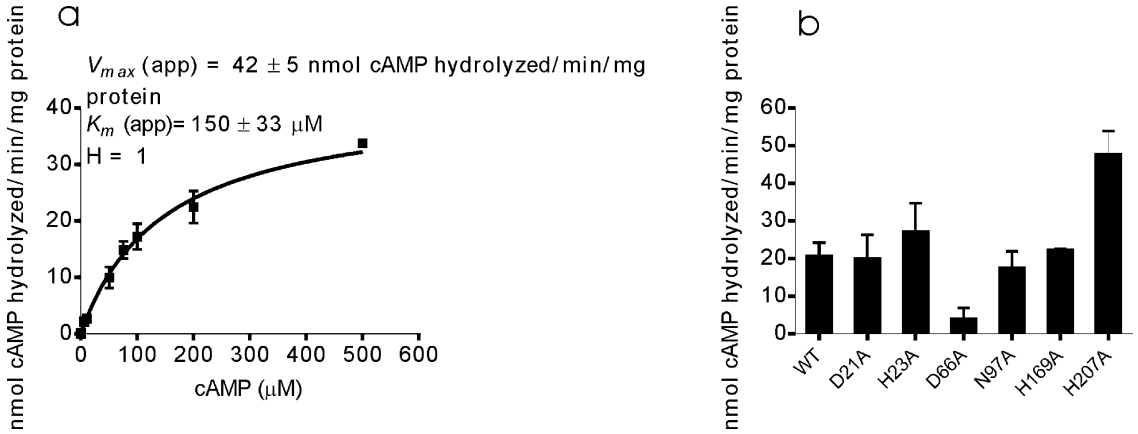

FIGURE 5: cAMP PDE activity of Rv0805. (a) Kinetic parameters of Rv0805 with respect to cAMP were estimated (~500 nM protein) in the presence of 100 μM Mn and indicated concentrations of cAMP as substrate. (b) Indicated mutant proteins (at ~500 nM) were assayed in the presence of ~500 μM cAMP in the presence of 100 μM Mn.

Rv0805 Hydrolyzes Intracellular cAMP in E. coli and M. smegmatis. The modest V_{max} observed in vitro for Rv0805 using cAMP as a substrate prompted us to monitor levels of cAMP intracellularly when Rv0805 was expressed in bacteria. Indeed, cAMP levels in *E. coli* cells overexpressing Rv0805 were markedly reduced while there was no alteration

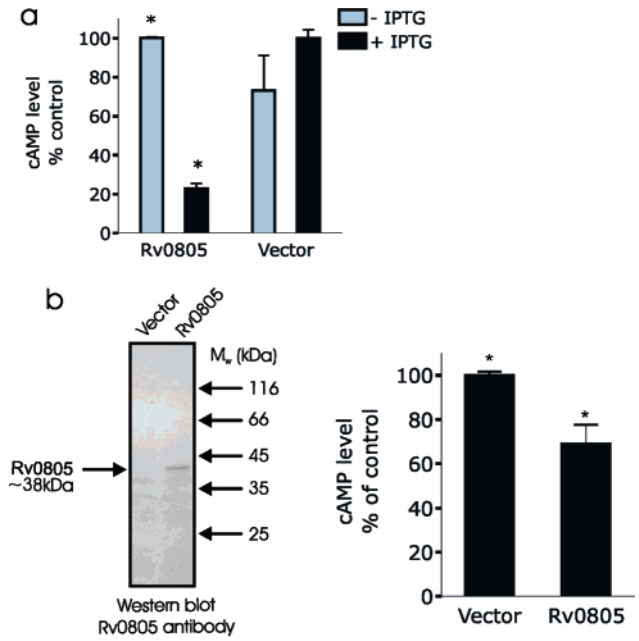

FIGURE 6: Activity of Rv0805 in vivo. (a) Intracellular cAMP levels were measured in *E. coli* transformed with empty vector or vector expressed Rv0805 under the inducible *trc* promoter, following addition of IPTG. cAMP levels reduce upon expression of Rv0805, with 100% = 200 pmol of cAMP/mg of protein. The asterisk indicates that the means are significantly different ($p < 0.005$) (b) Rv0805 was overexpressed in *M. smegmatis* under the control of the *hsp60* promoter, and intracellular cAMP levels were estimated by radioimmunoassay. Expression of Rv0805 was confirmed in lysates used for measuring cAMP by Western blot analysis using the affinity-purified Rv0805 antibody. The asterisk indicates that the means are significantly different ($p < 0.0001$), and 100% = 1000 pmol of cAMP/mg of protein.

in cAMP levels in cells transformed with vector alone or in the absence of IPTG (Figure 6a). These results indicate that Rv0805 is capable of hydrolyzing intracellular cAMP at physiological concentrations seen in *E. coli*.

M. smegmatis does not contain an orthologue of Rv0805. Constitutive expression of Rv0805 in *M. smegmatis* from a heat-shock promoter led to the synthesis of a protein corresponding to the size predicted for Rv0805, which could be detected on Western blot analysis using a specific antibody raised against Rv0805 (Figure 6b). Despite the levels of expression of Rv0805 being much lower than that seen in *E. coli*, expression of Rv0805 again led to a significant reduction in intracellular cAMP levels in *M. smegmatis* cells (Figure 6b), indicating that Rv0805 may regulate cAMP signaling in mycobacteria.

We do not detect significant levels of cGMP in lysates prepared from *E. coli* or *M. smegmatis*, in agreement with our prediction based on in silico analyses which could not detect guanylyl cyclases in mycobacteria (*39*). However, it is interesting to note that the recently characterized Rv1900c adenylyl cyclase from *M. tuberculosis* does show some guanylyl cyclase activity in vitro (*10*).

DISCUSSION

The results described here are the first detailed studies on a class III PDE which distinguishes these proteins from several characterized mammalian and plant MPEs. Rv0805 appears to be a protein that bound Fe and Mn as purified from *E. coli* with high affinity. It has been reported that Fe is present at 5-fold higher concentrations than Mn in *E. coli* cells (*40*), so it is possible that Rv0805 is picking up Fe fortuitously in the cell, since Fe alone was unable to support enzymatic activity in the absence of Mn. The *E. coli* CpdA was stimulated by $FeCl_2$ (*15*), but since 2,2′-dipyridyl did not affect the activity of Rv0805, Fe could be present in the Fe^{3+} form in Rv0805. Rv0805 was not expected to be inhibited by the inhibitors of class I PDEs due to the complete lack of similarity between these two classes of enzymes. However, Rv0805 was also not inhibited by free phosphate or pyrophosphate while some inhibition was observed with phosphotyrosine, which therefore suggests the presence of a hydrophobic binding pocket in the active site in which the phosphorylated phenol group [common to the bis(pNPP) substrate as well] binds. Perhaps this same region also allows for cyclic nucleotide binding. The λ phage serine/threonine phosphatase and PAPs have been shown to be inhibited by oxoanion analogues of phosphates (e.g., orthovanadate, molybdate, arsenate) (*41*, *42*). However, the 5′-nucleotidases are not inhibited by these compounds, indicating a difference in the active site and substrate binding of MPEs (*34*). It is also important to note that the difference in the protonation of active site histidine residues in Rv0805, due to its high pH optimum for enzymatic activity, might contribute to the differences in the properties of this enzyme as compared to other MPEs.

The bis(pNPP) substrate shows higher affinity for Rv0805 than the phosphodiesterase characterized from *Delftia* (*43*) (apparent K_m ~2.9 mM) and is comparable to that seen for an enzyme from *Burkholderia* (~0.9 mM) (*44*). The apparent K_m for the metal (Mn) is lower in the case of Rv0805 than that reported for Co^{2+} in the *E. coli* 5′-nucleotidase (*37*) (K_m of ~90 μM) and higher than that reported for the λ phosphatase (~6 μM) (*36*). Therefore, subtle modifications in the interaction of the metal ions and substrate, seen in the larger family of MPE proteins, could be further characterized with additional structural information on Rv0805.

Mutation of metal binding residues in Rv0805 resulted in a reduced affinity for Mn. Interestingly, this has also been observed in the case of mutants of similar residues in phospholipase D (a diesterase) from *Streptomyces chromofuscus* (*38*). Mutational studies of metal binding residues of the λ serine/threonine phosphatase have been carried out earlier (*36*), but though changes in the apparent K_m and V_{max} were observed, none of the mutants showed any cooperativity with respect to metal binding. The large difference in the Hill coefficients in Rv0805 with respect to Mn for D21A, H169A, D66A, and H207A mutants indicates a complicated interplay between the two metal binding sites and that the communication between them could involve these residues (Table 2). The modeled structure of Rv0805 reveals a potential hydrogen-bonding network between several residues at the active site, which could help in explaining some of the biochemical results obtained with mutant proteins. However, it is worth noting that most of the residues involved in hydrogen bonding are present in loop regions, and the difference in the lengths of loops in Rv0805 as compared to the PAP and Mre combined with the low sequence identity between these proteins (~16%) suggests that an alternate bonding pattern may be possible for at least some of the residues. This will become clear only upon solving the crystal structure of Rv0805.

The K_m of Rv0805 for cAMP is comparable to that reported for the enzyme from *E. coli* (~200 μM) (*15*). The utilization of cGMP as a substrate indicates the absence of strict cyclic nucleotide substrate specificity, again a property distinct from the *E. coli* CpdA which hydrolyzed only cAMP (*15*). It is therefore likely that the *M. tuberculosis* PDE during its course of evolution has gained the ability to hydrolyze both cyclic nucleotides, which it is likely to encounter during its obligate intracellular pathogenesis. Since cGMP is utilized extensively in eukaryotic signaling, it is conceivable that the homologues of Rv0805 found in mammals may also hydrolyze cGMP.

A number of microarray studies provide provocative suggestions that Rv0805 may have an important role to play in the physiology and pathobiology of *M. tuberculosis*. The Rv0805 RNA was induced ~1.5-fold upon treatment with the thiol-specific oxidizing agent, diamide, and the requirement of *sigH*, a σ factor involved in stress responses, appeared to be required for the transcription of Rv0805 (*45*). The Rv0805 transcript was downregulated during treatment with the drug isoniazid that is used for the treatment of tuberculosis (*46*). In a study on nutrient deprivation, Rv0805 was found to be induced maximally (~2-fold) on day 49 and was found to be repressed (~0.5-fold) on day 104 (*47*). Interestingly, expression levels were found to change upon oxygen deprivation, and Rv0805 expression levels were found to initially peak during the nonreplicating persistence phase up to day 8 (~3-fold as compared to cells in mid-log phase) and then reduce progressively up to day 80 (~0.07-fold) (*48*). Most interestingly, Rv0805 transcripts were found to be induced in mycobacteria isolated from both resting and activated wild-type macrophages (*49*). Since we have observed simultaneous expression of at least 15 of the 16 class III nucleotide cyclases in *M. tuberculosis* (Shenoy and Visweswariah, unpublished observations), it suggests that a detailed study on the regulation of expression of Rv0805 is warranted. The fact that Rv0805 is expressed at higher levels during mycobacterial infection points toward the possibility that intracellular cAMP levels in mycobacteria are likely to be low during interaction with the macrophage.

Since the intracellular levels of cAMP in mycobacteria are about 10-fold higher than that seen in *E. coli* (*50*), it is likely that Rv0805 plays an important role in regulating cAMP levels. Orthologues of Rv0805 are found only in *M. tuberculosis*, *M. bovis*, and, importantly, *M. leprae.* In addition to the degradation of cNMP, other mechanisms of reducing intracellular cAMP levels, for example, by secretion outside the cell, cannot be ruled out. We do in fact observe high levels of secreted cAMP in the culture medium of *M. smegmatis* (Shenoy and Visweswariah, unpublished observations).

Our computational and biochemical studies described here attribute a function to the Rv0805 gene, annotated as a *cpdA* homologue. Our studies have provided an additional regulatory aspect of cAMP signaling in this organism, since enzymes known to synthesize cyclic nucleotides have been characterized from Mycobacteria, and the results described here now provide evidence for the existence of a protein that could degrade both cAMP and cGMP. Indeed, Rv0805 represents another example of the presence of eukaryotic-like proteins in the mycobacterial genome, and our future efforts will focus on the structure and function(s) of this protein in pathogenic mycobacteria.

ACKNOWLEDGMENT

We thank Dr. Bob Kennedy, M. Dass, Achuth Padmanabhan, and Kajal Kanchan for technical assistance. Our thanks also go to Prof. John Kuriyan for a critical reading of the manuscript. We acknowledge the help of Prof. A. G. Samuelson, Department of Inorganic and Physical Chemistry, Indian Institute of Science, for useful discussions. Preliminary genomic sequence data for *M. avium* and *M. smegmatis* were made available from The Institute for Genomic Research (TIGR) website at http://www.tigr.org.

REFERENCES

1. Smith, C. V., Sharma, V., and Sacchettini, J. C. (2004) TB drug discovery: addressing issues of persistence and resistance, *Tuberculosis (Edinburgh) 84*, 45−55.
2. Cole, S. T., Brosch, R., Parkhill, J., Garnier, T., Churcher, C., Harris, D., Gordon, S. V., Eiglmeier, K., Gas, S., Barry, C. E., III, Tekaia, F., Badcock, K., Basham, D., Brown, D., Chillingworth, T., Connor, R., Davies, R., Devlin, K., Feltwell, T., Gentles, S., Hamlin, N., Holroyd, S., Hornsby, T., Jagels, K., Barrell, B. G., et al. (1998) Deciphering the biology of *Mycobacterium tuberculosis* from the complete genome sequence, *Nature 393*, 537−544.
3. McCue, L. A., McDonough, K. A., and Lawrence, C. E. (2000) Functional classification of cNMP-binding proteins and nucleotide cyclases with implications for novel regulatory pathways in *Mycobacterium tuberculosis*, *Genome Res. 10*, 204−219.
4. Shenoy, A. R., Sivakumar, K., Krupa, A., Srinivasan, N., and Visweswariah, S. S. (2004) A survey of nucleotide cyclases in Actinobacteria: unique domain organization and expansion of the class III cyclase family in *Mycobacterium tuberculosis*, *Comput. Funct. Genomics 5*, 17−38.
5. Linder, J. U., Hammer, A., and Schultz, J. E. (2004) The effect of HAMP domains on class IIIb adenylyl cyclases from *Mycobacterium tuberculosis*, *Eur. J. Biochem. 271*, 2446−2451.
6. Linder, J. U., and Schultz, J. E. (2003) The class III adenylyl cyclases: multi-purpose signalling modules, *Cell. Signalling 15*, 1081−1089.
7. Shenoy, A. R., Sreenath, N. P., Mahalingam, M., and Visweswariah, S. S. (2005) Characterization of phylogenetically distant members of the adenylyl cyclase family from mycobacteria: Rv1647 from *M. tuberculosis* and its ortholog ML1399 from *M. leprae*, *Biochem. J. 387*, 541−551.
8. Shenoy, A. R., Srinivas, A., Mahalingam, M., and Visweswariah, S. S. (2005) An adenylyl cyclase pseudogene in *Mycobacterium tuberculosis* has a functional ortholog in *Mycobacterium avium*, *Biochimie 87*, 557−563.
9. Shenoy, A. R., Srinivasan, N., Subramaniam, M., and Visweswariah, S. S. (2003) Mutational analysis of the *Mycobacterium tuberculosis* Rv1625c adenylyl cyclase: residues that confer nucleotide specificity contribute to dimerization, *FEBS Lett. 545*, 253−259.
10. Sinha, S. C., Wetterer, M., Sprang, S. R., Schultz, J. E., and Linder, J. U. (2005) Origin of asymmetry in adenylyl cyclases: structures of *Mycobacterium tuberculosis* Rv1900c, *EMBO J. 24*, 663−673.
11. Young, T. A., Delagoutte, B., Endrizzi, J. A., Falick, A. M., and Alber, T. (2003) Structure of *Mycobacterium tuberculosis* PknB supports a universal activation mechanism for Ser/Thr protein kinases, *Nat. Struct. Biol. 10*, 168−174.
12. Mehats, C., Andersen, C. B., Filopanti, M., Jin, S. L., and Conti, M. (2002) Cyclic nucleotide phosphodiesterases and their role in endocrine cell signaling, *Trends Endocrinol. Metab. 13*, 29−35.
13. Charbonneau, H. (1990) *Structure−function relationships among cyclic nucleotide phosphodiesterases*, Wiley, New York.
14. Richter, W. (2002) 3′,5′ Cyclic nucleotide phosphodiesterases class III: members, structure, and catalytic mechanism, *Proteins 46*, 278−286.
15. Imamura, R., Yamanaka, K., Ogura, T., Hiraga, S., Fujita, N., Ishihama, A., and Niki, H. (1996) Identification of the cpdA gene encoding cyclic 3′,5′-adenosine monophosphate phosphodiesterase in *Escherichia coli*, *J. Biol. Chem. 271*, 25423−25429.

16. Macfadyen, L. P., Ma, C., and Redfield, R. J. (1998) A 3′,5′ cyclic AMP (cAMP) phosphodiesterase modulates cAMP levels and optimizes competence in *Haemophilus influenzae* Rd, *J. Bacteriol. 180*, 4401−4405.
17. Goldberg, J., Huang, H. B., Kwon, Y. G., Greengard, P., Nairn, A. C., and Kuriyan, J. (1995) Three-dimensional structure of the catalytic subunit of protein serine/threonine phosphatase-1, *Nature 376*, 745−753.
18. Strater, N., Klabunde, T., Tucker, P., Witzel, H., and Krebs, B. (1995) Crystal structure of a purple acid phosphatase containing a dinuclear Fe(III)-Zn(II) active site, *Science 268*, 1489−1492.
19. Koonin, E. V. (1994) Conserved sequence pattern in a wide variety of phosphoesterases, *Protein Sci. 3*, 356−358.
20. Marchler-Bauer, A., Anderson, J. B., Cherukuri, P. F., DeWeese-Scott, C., Geer, L. Y., Gwadz, M., He, S., Hurwitz, D. I., Jackson, J. D., Ke, Z., Lanczycki, C. J., Liebert, C. A., Liu, C., Lu, F., Marchler, G. H., Mullokandov, M., Shoemaker, B. A., Simonyan, V., Song, J. S., Thiessen, P. A., Yamashita, R. A., Yin, J. J., Zhang, D., and Bryant, S. H. (2005) CDD: a conserved domain database for protein classification, *Nucleic Acids Res. 33* (Database Issue), D192−D196.
21. Bateman, A., Coin, L., Durbin, R., Finn, R. D., Hollich, V., Griffiths-Jones, S., Khanna, A., Marshall, M., Moxon, S., Sonnhammer, E. L., Studholme, D. J., Yeats, C., and Eddy, S. R. (2004) The Pfam protein families database, *Nucleic Acids Res. 32*, D138−D141.
22. Shenoy, A. R., and Visweswariah, S. S. (2003) Site-directed mutagenesis using a single mutagenic oligonucleotide and DpnI digestion of template DNA, *Anal. Biochem. 319*, 335−336.
23. Marti-Renom, M. A., Stuart, A. C., Fiser, A., Sanchez, R., Melo, F., and Sali, A. (2000) Comparative protein structure modeling of genes and genomes, *Annu. Rev. Biophys. Biomol. Struct. 29*, 291−325.
24. Kelley, L. A., MacCallum, R. M., and Sternberg, M. J. (2000) Enhanced genome annotation using structural profiles in the program 3D-PSSM, *J. Mol. Biol. 299*, 499−520.
25. Klabunde, T., Strater, N., Frohlich, R., Witzel, H., and Krebs, B. (1996) Mechanism of Fe(III)-Zn(II) purple acid phosphatase based on crystal structures, *J. Mol. Biol. 259*, 737−748.
26. Hopfner, K. P., Karcher, A., Craig, L., Woo, T. T., Carey, J. P., and Tainer, J. A. (2001) Structural biochemistry and interaction architecture of the DNA double-strand break repair Mre11 nuclease and Rad50 ATPase, *Cell 105*, 473−485.
27. Schenk, G., Gahan, L. R., Carrington, L. E., Mitic, N., Valizadeh, M., Hamilton, S. E., de Jersey, J., and Guddat, L. W. (2005) Phosphate forms an unusual tripodal complex with the Fe−Mn center of sweet potato purple acid phosphatase, *Proc. Natl. Acad. Sci. U.S.A. 102*, 273−278.
28. Guex, N., and Peitsch, M. C. (1997) SWISS-MODEL and the Swiss-PdbViewer: an environment for comparative protein modeling, *Electrophoresis 18*, 2714−2723.
29. Holm, L., and Park, J. (2000) DaliLite workbench for protein structure comparison, *Bioinformatics 16*, 566−567.
30. DasGupta, S. K., Jain, S., Kaushal, D., and Tyagi, A. K. (1998) Expression systems for study of mycobacterial gene regulation and development of recombinant BCG vaccines, *Biochem. Biophys. Res. Commun. 246*, 797−804.
31. Sassetti, C. M., Boyd, D. H., and Rubin, E. J. (2003) Genes required for mycobacterial growth defined by high-density mutagenesis, *Mol. Microbiol. 48*, 77−84.
32. Reiter, T. A., Reiter, N. J., and Rusnak, F. (2002) Mn^{2+} is a native metal ion activator for bacteriophage lambda protein phosphatase, *Biochemistry 41*, 15404−15409.
33. Guddat, L. W., McAlpine, A. S., Hume, D., Hamilton, S., de Jersey, J., and Martin, J. L. (1999) Crystal structure of mammalian purple acid phosphatase, *Struct. Folding Des. 7*, 757−767.
34. Knofel, T., and Strater, N. (2001) Mechanism of hydrolysis of phosphate esters by the dimetal center of 5′-nucleotidase based on crystal structures, *J. Mol. Biol. 309*, 239−254.
35. Egloff, M. P., Cohen, P. T., Reinemer, P., and Barford, D. (1995) Crystal structure of the catalytic subunit of human protein phosphatase 1 and its complex with tungstate, *J. Mol. Biol. 254*, 942−959.
36. Zhuo, S., Clemens, J. C., Stone, R. L., and Dixon, J. E. (1994) Mutational analysis of a Ser/Thr phosphatase. Identification of residues important in phosphoesterase substrate binding and catalysis, *J. Biol. Chem. 269*, 26234−26238.
37. McMillen, L., Beacham, I. R., and Burns, D. M. (2003) Cobalt activation of *Escherichia coli* 5′-nucleotidase is due to zinc ion displacement at only one of two metal-ion-binding sites, *Biochem. J. 372*, 625−630.
38. Zambonelli, C., Casali, M., and Roberts, M. F. (2003) Mutagenesis of putative catalytic and regulatory residues of *Streptomyces chromofuscus* phospholipase D differentially modifies phosphatase and phosphodiesterase activities, *J. Biol. Chem. 278*, 52282−52289.
39. Shenoy, A. R., and Visweswariah, S. S. (2004) Class III nucleotide cyclases in bacteria and archaebacteria: lineage-specific expansion of adenylyl cyclases and a dearth of guanylyl cyclases, *FEBS Lett. 561*, 11−21.
40. Posey, J. E., and Gherardini, F. C. (2000) Lack of a role for iron in the Lyme disease pathogen, *Science 288*, 1651−1653.
41. Reiter, N. J., White, D. J., and Rusnak, F. (2002) Inhibition of bacteriophage lambda protein phosphatase by organic and oxoanion inhibitors, *Biochemistry 41*, 1051−1059.
42. Crans, D. C., Simone, C. M., Holz, R. C., and Que, L., Jr. (1992) Interaction of porcine uterine fluid purple acid phosphatase with vanadate and vanadyl cation, *Biochemistry 31*, 11731−11739.
43. Tehara, S. K., and Keasling, J. D. (2003) Gene cloning, purification, and characterization of a phosphodiesterase from Delftia acidovorans, *Appl. Environ. Microbiol. 69*, 504−508.
44. Dotson, S. B., Smith, C. E., Ling, C. S., Barry, G. F., and Kishore, G. M. (1996) Identification, characterization, and cloning of a phosphonate monoester hydrolase from *Burkholderia caryophilli* PG2982, *J. Biol. Chem. 271*, 25754−25761.
45. Manganelli, R., Voskuil, M. I., Schoolnik, G. K., Dubnau, E., Gomez, M., and Smith, I. (2002) Role of the extracytoplasmic-function sigma factor sigma(H) in *Mycobacterium tuberculosis* global gene expression, *Mol. Microbiol. 45*, 365−374.
46. Waddell, S. J., Stabler, R. A., Laing, K., Kremer, L., Reynolds, R. C., and Besra, G. S. (2004) The use of microarray analysis to determine the gene expression profiles of *Mycobacterium tuberculosis* in response to anti-bacterial compounds, *Tuberculosis (Edinburgh) 84*, 263−274.
47. Hampshire, T., Soneji, S., Bacon, J., James, B. W., Hinds, J., Laing, K., Stabler, R. A., Marsh, P. D., and Butcher, P. D. (2004) Stationary phase gene expression of *Mycobacterium tuberculosis* following a progressive nutrient depletion: a model for persistent organisms?, *Tuberculosis (Edinburgh) 84*, 228−238.
48. Voskuil, M. I., Visconti, K. C., and Schoolnik, G. K. (2004) *Mycobacterium tuberculosis* gene expression during adaptation to stationary phase and low-oxygen dormancy, *Tuberculosis (Edinburgh) 84*, 218−227.
49. Schnappinger, D., Ehrt, S., Voskuil, M. I., Liu, Y., Mangan, J. A., Monahan, I. M., Dolganov, G., Efron, B., Butcher, P. D., Nathan, C., and Schoolnik, G. K. (2003) Transcriptional adaptation of *Mycobacterium tuberculosis* within macrophages: insights into the phagosomal environment, *J. Exp. Med. 198*, 693−704.
50. Padh, H., and Venkitasubramanian, T. A. (1976) Cyclic adenosine 3′,5′-monophosphate in mycobacteria, *Indian J. Biochem. Biophys. 13*, 413−414.

BI0512391